JOURNAL OF THEORETICAL AND APPLIED MECHANICS
51, 4, pp. 891-902, Warsaw 2013

GLOBAL BUCKLING PREVENTION CONDITION OF ALL-STEEL BUCKLING RESTRAINED BRACES

Nader Hoveidae, Behzad Rafezy
Sahand University of Technology, Faculty of Civil Engineering, Sahand, Tabriz, Iran
e-mail: hoveidae@gmail.com; nader.hoveidae@polymtl.ca; rafezyb@sut.ac.ir

One of the key requirements for the desirable mechanical behavior of buckling restrained braces (BRBs) under severe lateral loading is to prevent overall buckling until the brace member reaches sufficient plastic deformation and ductility. This paper presents finite element analysis results of proposed all-steel buckling restrained braces. The proposed BRBs have identical core sections but different Buckling Restraining Mechanisms (BRMs). The objective of the analyses is to conduct a parametric study of BRBs with different amounts of gaps and cores and BRM contact friction coefficients to investigate the global buckling behavior of the brace. The results of the analyses showed that BRM flexural stiffness could significantly affect the global buckling behavior of a BRB. However, the global buckling response occurred to be strongly dependent upon the magnitude of the friction coefficient between the core and the encasing contact surfaces. In addition, the results showed that the global buckling response of BRBs with direct contact of the core and BRM is more sensitive to the magnitude of contact friction coefficient.

Key words: all-steel buckling restrained brace, global buckling, finite element analysis, contact friction coefficient, cyclic loading

1. Introduction

Seismic excitations have led to concerns in structural design in earthquake-prone zones. During severe ground motion, large amount of kinetic energy is transmitted into a structure. Seismic codes and studies have been recognized that it is not economical to dissipate the seismic energy within the elastic capacity of materials and, as a consequence, it is preferable to anticipate yielding in some controlled elements. Braces are preliminary devices for energy absorption in braced buildings. However, buckling of the brace in compression results in sudden loss of stiffness, strength, and energy dissipation capacity. To overcome this deficiency, various types of innovations have been proposed in steel braces in which the buckling has been inhabited through a mechanism.

Buckling Restrained Braced Frames (BRBFs) have been widely used in recent years. A BRBF differs from a conventionally braced frame because it yields under both tension and compression without significant degradation in compressive capacity. Most buckling restrained brace (BRB) members currently available are built by inserting a steel plate into a steel tube filled with mortar or concrete called conventional BRBs. The steel plate is restrained laterally by the mortar or the steel tube and can yield in compression as well as tension, which results in comparable yield resistance and ductility as well as a stable hysteretic behavior in BRBs. A large body of knowledge exists on conventional BRBs performance in the literature. Black *et al.* (2002) performed component testing of BRBs and modeled a hysteretic curve to compare the test results, and found that the hysteretic curve of a BRB is stable, symmetrical, and ample. Inoue *et al.*(2001) introduced buckling restrained braces as hysteretic dampers to enhance the seismic response of building structures. As shown in Fig. 1, a typical BRB member consists

of a steel core, a buckling restraining mechanism (BRM), and a separation gap or unbonding agent allowing independent axial deformation of the inner core relative to the BRM. Numerous researchers have conducted experiments and numerical analyses on BRBs for incorporation into seismic force resisting systems. Qiang (2005) investigated the use of BRBs for practical applications for buildings in Asia. Clark *et al.* (1999) suggested a design procedure for buildings incorporating BRBs. Sabelli *et al.* (2003) reported seismic demands on BRBs through a seismic response analysis of BRB frames, and Fahnestock *et al.* (2007) conducted a numerical analysis and pseudo dynamic experiments of large-scale BRB frames in the U.S.

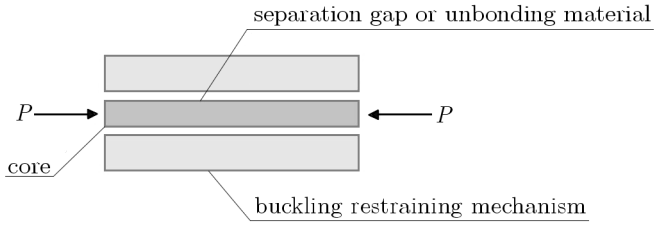

Fig. 1. Components of a BRB

The local buckling behavior of BRBs was studied by Takeuchi *et al.* (2005). The effective buckling load of BRBs considering the stiffness of the end connection was recently studied by Tembata *et al.* (2004) and Kinoshita *et al.*(2007). Previous studies have demonstrated the potential of manufacturing BRB systems made entirely of steel, called all-steel BRBs (Tremblay *et al.*, 2006). In a conventional all-steel BRB, the steel inner core is sandwiched with a buckling restraining mechanism made entirely of steel components, thus avoiding the costs of the mortar needed in conventional BRBs. This eliminates the fabrication steps associated with pouring and curing the mortar or concrete, significantly reducing manufacturing time and costs. In addition, such a BRB can be easily disassembled for inspection after an earthquake. Experimental and analytical studies on the deformation performance and dynamic response of BRBs were performed by Kato *et al.* (2002), Watanabe *et al.* (2003), and Usami (2006). The restraining member proposed previously was a mortar-filled steel section, which made an extremely rigid member. In such types of BRBs, the brace member and the BRM were integrated, and overall buckling did not occur. However, in all-steel BRBs, which are considered to be a new generation of buckling restrained braces, the brace system is made completely of steel, and the BRM system is lighter in comparison with conventional BRBs, which leads to a high potential for brace overall buckling caused by the low rigidity and stiffness of the BRM. The hysteretic behavior of all-steel BRBs was experimentally investigated by Tremblay *et al.* (2006). An experimental study on the hysteretic response of all-steel BRBs was also conducted by Eryasar and Topkaya (2010).

The following characteristics are considered necessary for the safe performance of BRBs: 1) the prevention of overall buckling, 2) the prevention of core local buckling, 3) the prevention of low cycle fatigue of the brace member, and 4) high strength of the joint parts and connections. In this paper, the first characteristic (i.e., overall buckling behavior) is examined further.

Assume a BRB member with initial deflection under compression. When the inner core with initial inherent imperfection deflects under compression, it comes into contact with the BRM. The contact forces increase the out-of-plane deformation of the entire BRB and strength deterioration occurs before the brace member reaches the target displacement if the rigidity and strength of the BRM are insufficient. According to the AISC 2005 guidelines for qualifying cyclic tests of BRBs (AISC 2005), a BRB should undergo axial deformations up to Δ_{bm}, where Δ_{bm} is the brace axial deformation corresponding to the design story drift. The buckling restraining component should have enough strength and rigidity to prevent overall buckling of the brace during axial deformation. Therefore, to obtain the hysteretic characteristic on the compression side similar to that on the tension side and to mitigate pinching, it becomes necessary to avoid

overall buckling (i.e., flexural buckling). The results of the first studies on overall buckling behavior of BRBs conducted by Watanabe *et al.* revealed that the ratio of Euler buckling load of the restraining member to the yield strength of the core, P_e/P_y, is the factor that is the most determinative for control of brace global buckling(Watanabe *et al.*, 1988). These authors concluded that if the ratio of the Euler buckling load of the BRM to the yield load of the inner core, P_e/P_y, is less than one, the brace member will experience overall buckling during cyclic loading of the braced frame. However, a P_e/P_y ratio of 1.5 was proposed for design purposes in the studies mentioned. The criterion $P_e/P_y \geqslant 1$ has a theoretical basis (Black *et al.*, 2002) and has been verified through experimental testing (Iwata and Murai, 2006). However, the aforementioned studies did not consider the contact properties between the core and the encasing. In other words, the friction coefficient of the core and the encasing contact surface was not considered as an affecting parameter that might change the overall buckling prevention condition of a BRB. More experimental studies were conducted by Usami (2006) on all-steel BRBs and a safety factor of $\lambda_f = P_{max}/P_y$ was proposed where P_{max} and P_y denote the maximum compression force in the brace member and the core yielding capacity, respectively. The safety factor is illustrated as follows

$$\gamma_f = \frac{1}{\frac{P_y}{P_e} + \frac{P_y}{M_y}(a+d+e)} \tag{1.1}$$

where a, d and e are the initial deflection, gap amplitude, and the eccentricity of loading, respectively. Test results showed that if the value of safety factor γ_f was greater than three, overall buckling of BRB would not occur.

The finite element analysis method was recently used with success to predict the buckling response of the core plates in BRB members with tubes filled with mortar (Matsui *et al.*, 2008). Subsequent finite element analysis studies have been conducted by Korzekwa and Tremblay (2009) to investigate the core buckling behavior in all-steel BRBs. The studies mentioned above also provided a description of the complex interaction that develops between the brace core and BRM. Outward forces induced by the contact forces were found to be resisted in flexure by the BRM components and in the bolts holding together the BRM components located on each side of the core. In addition, the contact forces resulted in longitudinal frictional forces that induced axial compression loads in the BRM. The representative P_e/P_y ratio used in these studies was 3.5, and the test results showed that the encasing strength was adequate to prevent global buckling of the brace.

This paper numerically investigates the overall buckling inhibition condition of all-steel BRBs regarding the effect of gap size and the friction coefficient magnitude of the contact between the core and the buckling restraining mechanism.

2. Overall buckling prevention criterion of BRBs

Analysis of elastic buckling of a BRB composed of a steel core restrained laterally by a BRM showed that the Euler buckling load of the brace member under compression could be found by solving an equilibrium equation as follows (Fujimoto *et al.*, 1988)

$$E_B I_B \frac{d^2 v}{dx^2} + (v + v_0) N_{max} = 0 \tag{2.1}$$

in which $E_B I_B$ is the flexural stiffness of the BRM, N_{max} represents the maximum brace axial load, and v and v_0 denote the transverse and the initial deflection of the brace member, respectively, as shown in Fig. 2.

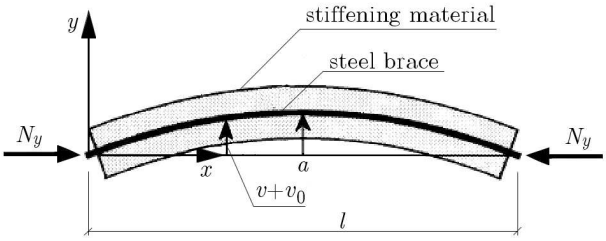

Fig. 2. Force and deformation of a BRB (Qiang, 2005)

The initial deflection of the brace is assumed to be expressed by a sinusoidal curve as follows

$$v_0 = a \sin \frac{\pi x}{L} \tag{2.2}$$

where a is the initial deflection of the brace at the center and N is the brace axial load, which is replaced with P in the following equations. Solving equilibrium Eq. (2.1) results in the following

$$v + v_0 = \frac{a}{1 - \frac{P_{max}}{P_e}} \sin \frac{\pi x}{L} \tag{2.3}$$

The bending moment at the center of BRM can be written as follows

$$M_c = \frac{P_{max} a}{1 - \frac{P_{max}}{P_e}} \tag{2.4}$$

where P_{max} is the maximum axial force of the brace. Assuming that P_{max} is equal to P_y (i.e., yield load of the core) and considering that the buckling of the BRB occurs when the maximum stress in the outermost fiber of the BRM reaches the yield stress, the requirement for stiffness and strength of the steel tube (BRM) can be obtained as follows

$$\frac{P_e}{P_y} \geqslant 1 + \frac{\pi^2 E_B a D}{2\sigma_y L_B^2} \tag{2.5}$$

in which L_B, σ_y, and D denote the length, the yield stress of the steel tube, and the depth of the restraining member section, respectively. This is the first formula that successfully expresses strength and stiffness requirements as paired in the design of BRBs. In this formula, the effect of gap amplitude g has not been considered in the calculation of the moment at the center of the BRM (Qiang 2005). Therefore, in this paper, this parameter is involved in Eq. (2.5). Thus, Eq. (2.5) can be modified as follows

$$\frac{P_e}{P_y} \geqslant 1 + \frac{\pi^2 E_B (a+g) D}{2\sigma_y L_B^2} = \beta \tag{2.6}$$

where L_B is the length of the core and BRM (equal together), and D s the depth of the BRM section. Equation (2.6) indicates that overall buckling of the brace will not occur if the ratio P_e/P_y is greater than the parameter β, which is calculated based on the geometric and material characteristics of the brace member.

3. Finite element analysis

To provide a numerical understanding of the cyclic behavior and buckling response of all-steel BRBs, a series of finite element analyses were conducted on 24 proposed all-steel BRBs. A three-dimensional representation of the brace specimens was developed to properly capture the expected behavior. The models included the core plates, and the BRM components consist of tubes, guide plates, filler plates, and end stiffeners.

3.1. Description of the models

Finite element analyses have been conducted on 24 proposed all-steel BRBs. Table 1 represents the details and specifications of the models where the second column shows the specimen code in the form $S(i)g(j)c(k)$, in which the indexes i, j, and k represent the model number, the gap amplitude, and the friction coefficient magnitude at the interface, respectively. All of the models consisted of a constant 100 mm×10 mm core plate with various cross sections for BRM members, as shown in Table 1. Therefore, the yield strength of the core was kept constant when the stiffness and strength of the BRMs were altered. The total length of the BRBs, L, was assumed to be 2000 mm. The core plate yield load, P_{yc}, which is illustrated by P_y, was calculated by multiplying the yield stress by the cross-sectional area, and the buckling load of the BRM, P_e, was calculated from the Euler buckling load formula. The dimensions of the brace components were selected in a way that the ratio of the Euler buckling load and the yield load of the brace in the specimens, P_e/P_y, falls between 1.09 and 2.60. The parameter I_r in Table 1 denotes the moment of inertia of the restraining member.

Table 1. Properties of BRB specimens

No.	Model name	BRM section dimensions [mm]	Core dimensions [mm]	A_c [mm^2]	Gap [mm]	I_r [mm^4]	P_e [KN]	P_{yc} [KN]
1	S1g0c0.1	UNP50+2Fp(45×5)	P-100×10	1000	0	81.46E+4	401.99	370
2	S2g0c0.1	UNP65+2Fp(37.5×5)	P-100×10	1000	0	111.84E+4	551.91	370
3	S3g0c0.1	B(50×50×3)+2Fp(45×5)	P-100×10	1000	0	148.46E+4	732.62	370
4	S4g0c0.1	B(50×50×4)+2Fp(45×5)	P-100×10	1000	0	190.00E+4	937.61	370
5	S1g0c0.3	UNP50+2Fp(45×5)	P-100×10	1000	0	81.46E+4	401.99	370
6	S2g0c0.3	UNP65+2Fp(37.5×5)	P-100×10	1000	0	111.84E+4	551.91	370
7	S3g0c0.3	B(50×50×3)+2Fp(45×5)	P-100×10	1000	0	148.46E+4	732.62	370
8	S4g0c0.3	B(50×50×4)+2Fp(45×5)	P-100×10	1000	0	190.00E+4	937.61	370
9	S1g0c0.5	UNP50+2Fp(45×5)	P-100×10	1000	0	81.46E+4	401.99	370
10	S2g0c0.5	UNP65+2Fp(37.5×5)	P-100×10	1000	0	111.84E+4	551.91	370
11	S3g0c0.5	B(50×50×3)+2Fp(45×5)	P-100×10	1000	0	148.46E+4	732.62	370
12	S4g0c0.5	B(50×50×4)+2Fp(45×5)	P-100×10	1000	0	190.00E+4	937.61	370
13	S1g1c0.1	UNP50+2Fp(45×5)	P-100×10	1000	1	85.00E+4	419.46	370
14	S2g1c0.1	UNP65+2Fp(37.5×5)	P-100×10	1000	1	116.00E+4	572.44	370
15	S3g1c0.1	B(50×50×3)+2Fp(45×5)	P-100×10	1000	1	152.60E+4	753.05	370
16	S4g1c0.1	B(50×50×4)+2Fp(45×5)	P-100×10	1000	1	195.23E+4	963.42	370
17	S1g1c0.3	UNP50+2Fp(45×5)	P-100×10	1000	1	85.00E+4	419.46	370
18	S2g1c0.3	UNP65+2Fp(37.5×5)	P-100×10	1000	1	116.00E+4	572.44	370
19	S3g1c0.3	B(50×50×3)+2Fp(45×5)	P-100×10	1000	1	152.60E+4	753.05	370
20	S4g1c0.3	B(50×50×4)+2Fp(45×5)	P-100×10	1000	1	195.23E+4	963.42	370
21	S1g1c0.5	UNP50+2Fp(45×5)	P-100×10	1000	1	85.00E+4	419.46	370
22	S2g1c0.5	UNP65+2Fp(37.5×5)	P-100×10	1000	1	116.00E+4	572.44	370
23	S3g1c0.5	B(50×50×3)+2Fp(45×5)	P-100×10	1000	1	152.60E+4	753.05	370
24	S4g1c0.5	B(50×50×4)+2Fp(45×5)	P-100×10	1000	1	195.23E+4	963.42	370

B – BOX; Fp – Face plate; P – Plate

The core plate and BRM was modeled using 8-node C3D8 brick elements. Large displacement static cyclic analysis was performed using the ABAQUS 6.9.3 (2005) general-purpose finite element program. The core plate was expected to undergo large plastic deformations and higher mode buckling with pronounced curvature. Therefore, a refined mesh was adopted with five elements across the plate and two over the thickness. A coarser mesh was used for the BRM because

most of this component was expected to remain elastic. Contact properties with hard stiffness in the transverse direction and tangential coulomb frictional behavior were assumed between the core and the BRM. Regarding studies in the field (Chou and Chen, 2010), a coefficient of friction of 0.1 was adopted to provide a greasy interface between the core and the BRM in the models. In addition friction coefficients of 0.3 (Korzekwa and Tremblay, 2009) and 0.5 were also adopted to provide a smooth and rough steel-to-steel contact surfaces between the core and the encasing, respectively. The contact model allowed for the separation of the core plate from the BRM element, which enabled the higher mode buckling of the core plate.

The core plate and the BRM components were made of steel with a yield stress of $F_y = 370\,\text{MPa}$. Young's modulus of $200\,\text{GPa}$ and Poisson's ratio of 0.3 were assumed for the core plate and the BRM components. A nonlinear combined isotropic-kinematic hardening rule was employed to reproduce the inelastic material property and, therefore, accurate cyclic behavior. The initial kinematic hardening modulus C and the rate factor γ were assumed to be $8\,\text{KN/mm}^2$ and 75, respectively (Korzekwa and Tremblay, 2009). For isotropic hardening, a maximum change in yield stress of $Q_\infty = 110\,\text{MPa}$ and a rate factor of $b = 4$ were adopted. An initial imperfection of 2 mm (i.e., $L/1000$) was considered in both the core plate and the BRM. Two types of interfaces between the core plate and BRM were considered in the models. In the first case, direct contact of the core plate with the BRM was implemented, and in the second case, gap amplitudes of 1 mm were provided through the core thickness. In addition, a constant gap amplitude of 2 mm was provided through the core width (on both sides) in all models. Such a gap was used to accommodate the free expansion of the inner core under axial loads. The axial deformation was blocked at one end of bracing with a pinned connection. Axial displacements were imposed at the other end following the cyclic quasi static protocol suggested by AISC seismic provisions for BRBs (2005) as follows: 2 cycles at $\pm\Delta_y$, 2 cycles at $\pm 0.5\Delta_{bm}$, 2 cycles at $\pm\Delta_{bm}$, 2 cycles at $\pm 1.5\Delta_{bm}$, and 2 cycles at $\pm 2\Delta_{bm}$, where Δ_y is the displacement that corresponds to the yielding of the core, and Δ_{bm} is the axial deformation of the brace corresponding to the design story drift. Based on the previous studies by Tremblay *et al.* (2006), the peak strain amplitude in full-length core braces typically falls in the range of 0.01 to 0.02 for common structural applications, and the peak deformation in the majority of past test programs have been limited to that range (Watanabe *et al.*, 1988). In this study, Δ_{bm} was set to 20 mm, which corresponds to the axial strain of 1% in the core, and the core yielding displacement Δ_y was calculated as 3.7 mm based on the material characteristics. Therefore, the ultimate axial displacement demand of the brace during cyclic loading will be $2\Delta_{bm} = 40\,\text{mm}$, which corresponds to a core strain of 2%. Therefore, the adopted value for the peak strain demand of the inner core seems reasonable. A typical cross section of the proposed BRB member and its finite element representation are shown in Figs. 3 and 4, respectively.

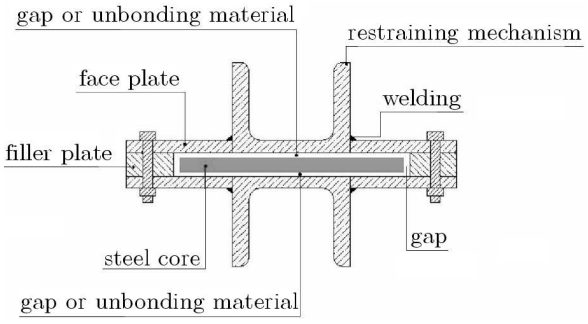

Fig. 3. Typical cross section of proposed BRBs

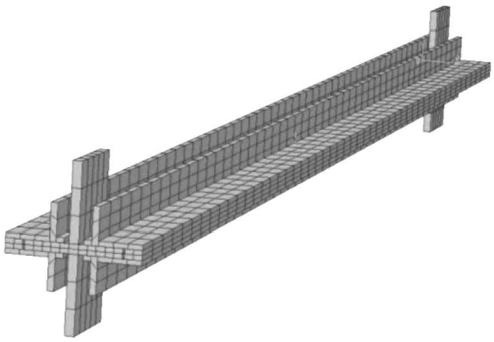

Fig. 4. Finite element model of a proposed BRB

4. Results and discussions

Hysteretic responses in all of the BRB models are well predicted by the finite element model in both elastic and nonlinear ranges. Figuree 5 and 6 illustrate the normalized hysteretic responses of the braces. In the curves, compression is positive.

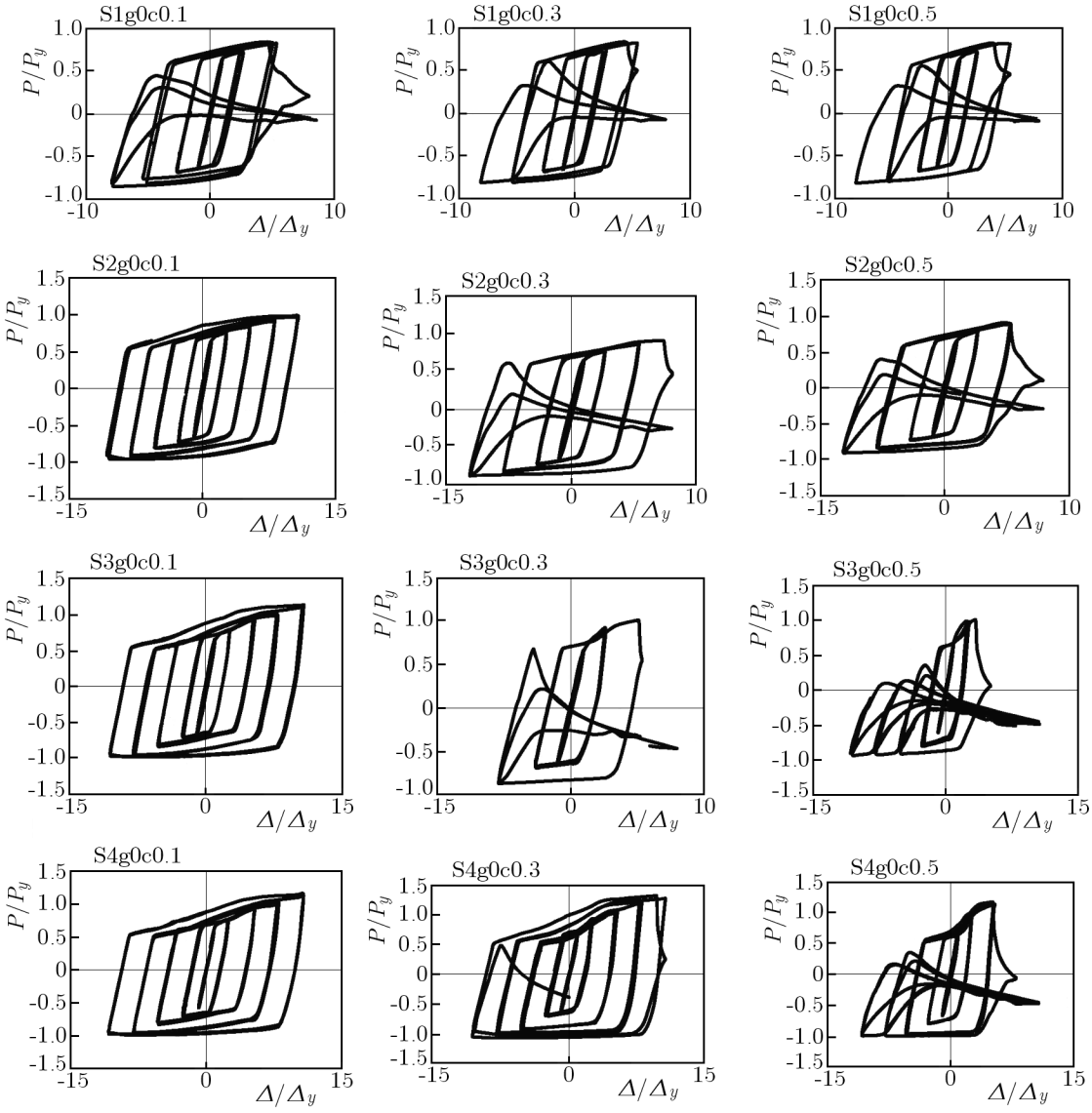

Fig. 5. Hysteretic responses of the proposed BRBs including direct contact of the core and BRM

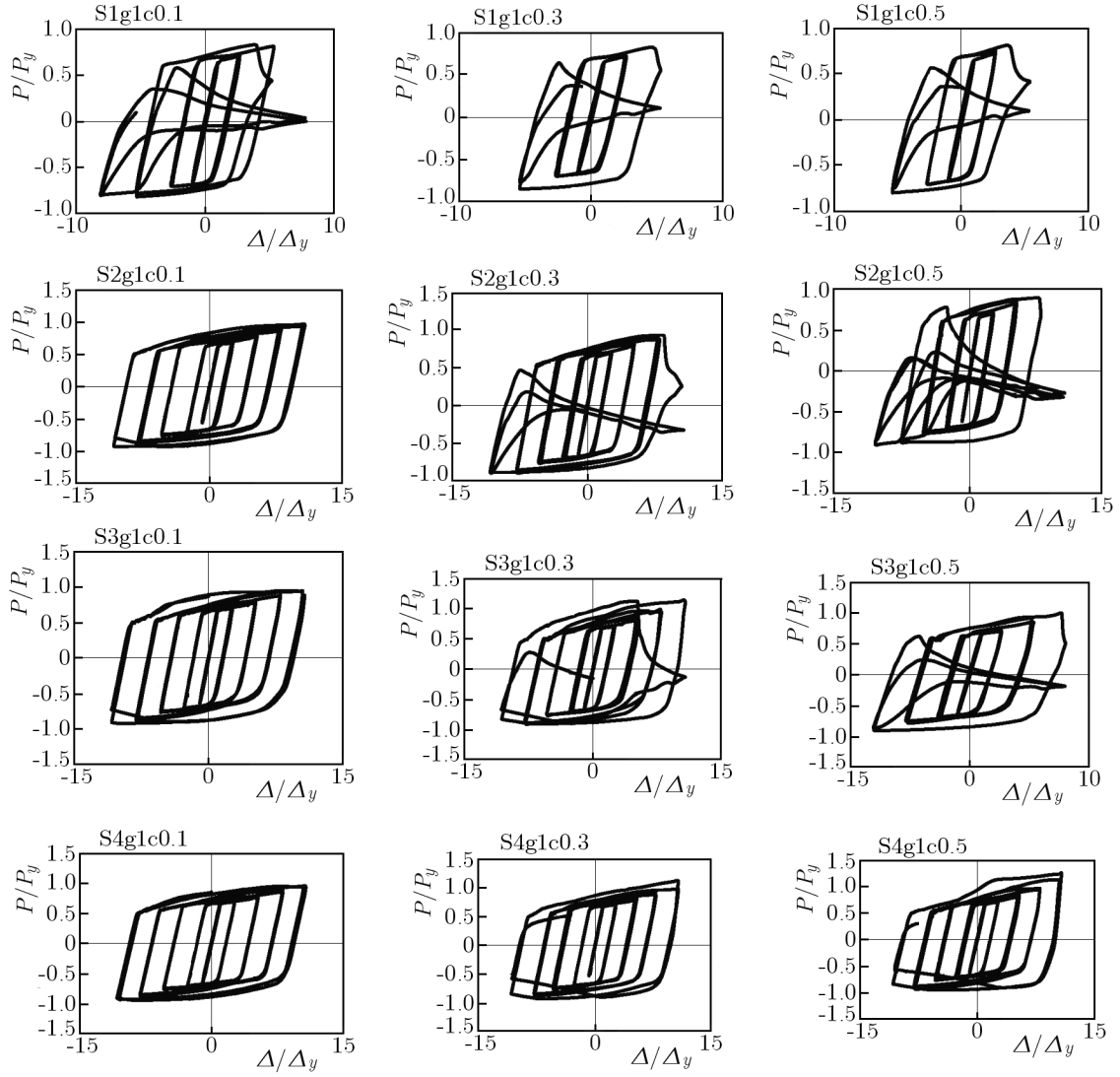

Fig. 6. Hysteretic responses of the proposed BRBs including a gap between the core and BRM

Axial force-displacement curves of the BRB models are captured from a point at the brace end. This point is located in a region that essentially remains elastic because stiffener plates are provided to prevent local buckling in the brace end. Therefore, the captured force-displacement relation may not be a representation of the true stress distribution of the core during cyclic loading, although the curves properly describe the deterioration in strength caused by the global or local buckling of the brace. The axial force-deformation curves shown in Figs. 5 and 6 indicate the sudden deterioration in the strength and overall buckling only in the models S1g0c0.1 and S1g1c0.1 with lower values of P_e/P_y among the models with the friction coefficient of 0.1 at the interface, whereas, in all of the other models with friction coefficient of 0.1, the stable hysteretic response without a significant change in the brace load carrying capacity is specified. In addition, in the similar models with the friction coefficients of 0.3 and 0.5, a premature overall buckling is observed which can be deducted from the hysteretic curves in Figs. 5 and 6. All of the models including direct contact with the friction coefficients of 0.3 and 0.5 experience global buckling during a cyclic loading up to $2\Delta_{bm}$ as shown in Figs. 5 and 6. In addition, all of the models with the friction coefficient of 0.3 and 0.5 and containing a gap size of 1 mm through the core thickness experience overall buckling except models S4g1c0.3 and S4g1c0.5 with larger strength and stiffness of BRM. The buckled shape of the brace is represented in Fig. 7a. The values of

P_e/P_y have been calculated for all 24 BRB specimens and are given in Table 2. In addition, the representative parameter β is calculated and shown in Table 2.

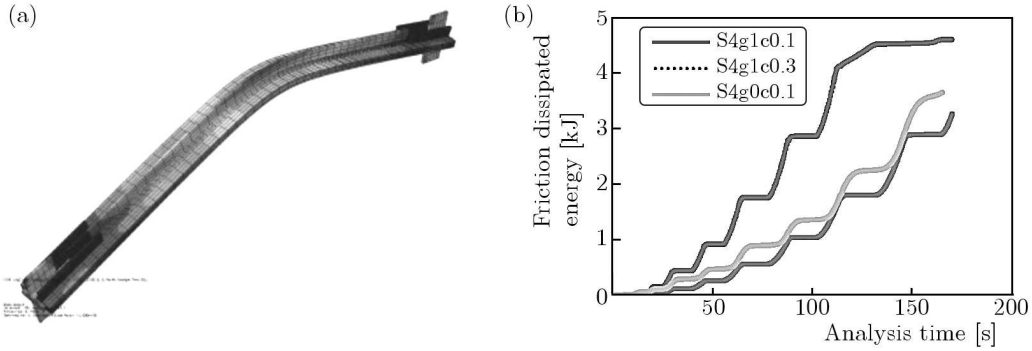

Fig. 7. (a) Overall buckling of model S1g0c0.1; (b) comparison of frictional dissipated energy in model S4g1c0.1, S4g1c0.3, and S4g0c0.1

Table 2. Analytical results for the proposed BRBs

No.	Model name	$\alpha = \frac{P_e}{P_y}$	β [8]	Global buckling
1	S1g0c0.1	1.09	1.11	Yes
2	S2g0c0.1	1.49	1.13	No
3	S3g0c0.1	1.98	1.15	No
4	S4g0c0.1	2.53	1.15	No
5	S1g0c0.3	1.09	1.11	Yes
6	S2g0c0.3	1.49	1.13	Yes
7	S3g0c0.3	1.98	1.15	Yes
8	S4g0c0.3	2.53	1.15	Yes
9	S1g0c0.5	1.09	1.11	Yes
10	S2g0c0.5	1.49	1.13	Yes
11	S3g0c0.5	1.98	1.15	Yes
12	S4g0c0.5	2.53	1.15	Yes
13	S1g1c0.1	1.13	1.24	Yes
14	S2g1c0.1	1.55	1.26	No
15	S3g1c0.1	2.04	1.30	No
16	S4g1c0.1	2.60	1.30	No
17	S1g1c0.3	1.13	1.24	Yes
18	S2g1c0.3	1.55	1.26	Yes
19	S3g1c0.3	2.04	1.30	Yes
20	S4g1c0.3	2.60	1.30	No
21	S1g1c0.5	1.13	1.24	Yes
22	S2g1c0.5	1.55	1.26	Yes
23	S3g1c0.5	2.04	1.30	Yes
24	S4g1c0.5	2.60	1.30	No

[8] – Fujimoto *et al.* (1988)

Based on the results of analysis and as shown in Table 2, models with a P_e/P_y ratio greater than 1.2 and the friction coefficient of 0.1 do not experience overall buckling during axial loading up to a core strain of 2%. In addition, in these models, the P_e/P_y ratio is greater than the parameter β. Therefore, the analysis results confirm the validity of Eq. (2.6). Moreover, the buckling prevention condition (i.e. $P_e/P_y \geqslant 1.2$) is not dependent on the gap size between the core and the encasing member in the models with the friction coefficient of 0.1. Table 2 shows

that the models with higher friction coefficients, such as 0.3 or 0.5, and including a direct contact of the core and the BRM experience global buckling despite of owning a larger P_e/P_y ratio such as 2.53. In addition, the models with the friction coefficients of 0.3 and 0.5 and containing a gap of 1 mm at the interface endure overall buckling when the P_e/P_y ratio is less than 2.6. The reason is that, in the models with higher friction coefficient, the slippage of the steel core inside the BRM does not occur freely and the applied axial displacement causes the brace (with initial imperfection) to deform laterally instead of free axial deformation.

In addition, a part of frictional forces developed at the interface is transmitted into the BRM, which causes the lateral deflection of the brace because of P-Δ effects. Therefore, the overall buckling behavior of the BRB members is dependent on the brace interface detail properties especially the magnitude of the friction coefficient. Frictional dissipated energy in models S4g1c0.1, S4g1c0.3, and S4g0c0.1 is compared together in Fig. 7b. As shown in Fig. 7b, the BRB with the direct contact of the core and BRM own larger frictional dissipated energy in comparison to the BRB including the gap. In addition, the frictional dissipated energy in the BRB model with the higher friction coefficient is larger.

During cyclic loading of a BRB member containing a gap between the core and the encasing, the brace member causes lateral deflection as the compressive displacement increases and the lateral deflection rises. Contact forces acting on the upper side of the BRM increase, and buckling of the brace member occurs when the moment at the center of the BRM as a result of the contact forces reaches the yield moment of the BRM. In models containing the gap, the lateral deflection rises to deformation of higher order buckling modes while enforcing compression displacement. The contact forces acting on both sides of the restraining member increase under compression and cause global buckling of the brace. The results show that the models with a P_e/P_y ratio greater than 1.2 and the friction coefficient of 0.1 do not experience global buckling regardless of the size of the gap. While loading the BRBs including the gap, severe inelastic excursions occur in the core plate under compression, which induces lateral opening of the BRM member. Previous studies conducted by Korzekwa and Tremblay (2009) also confirm this phenomenon. The results show that the overall buckling behavior of BRB models with direct contact of the core and the BRM is more sensitive to frictional response at the interface. In the other words, in the models without a gap at the interface, the frictional forces developed between the core and the encasing contact surface are considerably larger in comparison to those in the models including the gap. The excessive frictional forces generated at the interface result in the large axial force transmission into the BRM, the development of bending moments in the BRM, and the overall buckling of the entire brace, consequently.

Based on the results, the overall buckling behavior of BRBs depends on the interface detail properties. The known parameter P_e/P_y and the magnitude of friction coefficient at the core and the BRM interface are the most effective parameters that influence the overall buckling response of a BRB. Employing an unbonding material such as butyl rubber at the interface provides a surface with a friction coefficient near 0.1. In this case, the overall buckling prevention condition of the brace can be similar to the criterion suggested by previous researchers (i.e., $P_e/P_y \geqslant 1$)(Watanabe *et al.*, 1988). However, further numerical studies and experimental tests are necessary to examine and suggest guidelines on the overall buckling prevention condition and the design of all-steel BRBs with different interface details and various amounts of friction coefficients at the interface, consequently.

5. Conclusions

One of the key requirements of buckling restrained braces is the performance of avoiding overall buckling until the brace member reaches target displacement and sufficient ductility. This required performance becomes important as the BRB is lightened, and the strength and rigi-

dity of the restraining member are reduced. A new generation of BRBs, called all-steel BRBs, is a class of BRBs with lighter buckling restraining components than conventional BRBs. In this family of BRBs, a light steel component is used as a restraining member instead of the mortar-filled tubes used in conventional BRBs, which may result in overall buckling of the brace caused by inadequate rigidity and strength of the restraining components. In this paper, the overall buckling prevention condition of all-steel BRBs considering the core and the encasing interface detail is numerically examined through the finite element analysis method. Among 24 proposed all-steel BRB specimens, the models with friction coefficient of 0.1 and a P_e/P_y ratio less than 1.2 experienced global buckling during cyclic loading of the brace up to a core strain of 2%, which closely meets the overall buckling avoidance condition of BRBs suggested by previous researchers. However, larger P_e/P_y ratios are required to prevent overall buckling of the brace as the friction coefficient between core and BRM is increased.

The main out-com of the study can be summarized as follows:

- Results of analysis show that for the BRM component a larger strength and stiffness is required to inhibit global buckling of the brace when a higher friction coefficient or a rough surface is specified at the core and BRM interface. The known global buckling prevention condition of BRBs, $P_e/P_y > 1.2$, can be applied only for braces with smooth surfaces between the core and BRM and smaller friction coefficients, such as 0.1 and lower.
- The overall buckling response of the BRB is so sensitive to the magnitude of friction coefficient at the interface in the case with direct contact between the core and the BRM. In other words, the overall buckling of BRB with direct contact between at the interface corresponds to larger values of P_e/P_y in comparison to the models including a gap since the frictional forces developed at the interface in BRBs with direct contact of the core and BRM are higher in comparison to the BRBs including the gap. This leads to transmission of higher axial forces into the BRM and bending of the entire brace because of P-Δ effects.
- It is recommended to use an unbonding material at the core and BRM interface to reduce frictional forces and avoid premature overall buckling of BRBs. In addition, employing a gap between the core and BRM not only provides enough space to accommodate free lateral expansion of the core but also decreases the frictional forces and the chance of global buckling of the brace for a constant stiffness and strength of the BRM as a result. In addition, the cost of using such a material is low in comparison to the overall cost of fabrication of a BRB. However, although using a rough material between the core and BRM increases the magnitude of friction forces at the interface which may cause premature buckling of the BRB member; it noticeably increases the energy dissipation capacity of the brace by friction.
- The global buckling condition of a BRB is dependent on the interface characteristics such as the magnitude of the friction coefficient at the interface and the gap size. Further extensive experimental and numerical studies are required to survey and suggest the overall buckling prevention condition of all-steel BRBs for design purposes considering the interface properties, especially the contact characteristics between the core and the encasing member.

References

1. ABAQUS, Standard user's manual version 6.3, 2005, Pawtucket, RI: Hibbitt, Karlsson & Sorensen, Inc.
2. AISC (American Institute of Steel Construction), 2005, Seismic provisions for structural steel buildings, Chicago, IL

3. Black C.J., Makris N., Aiken I.D., 2002, Component Testing, Stability Analysis, and Characterization of Buckling Restrained Braced Frames, Report No. PEER 2002/08, California, Berkeley, CA
4. Chou C., Chen S., 2010, Sub-assemblage tests and finite element analyses of sandwiched buckling restrained braces, *Engineering Structures*, **32**, 2108-2121
5. Clark P., Aiken I., Kasai K., Ko E., Kimura I., 1999, Design procedures for buildings incorporating hysteretic damping devices, *Proceedings of 69th Annual Convention, SEAOC*, Sacramento, USA
6. Eryasar M., Topkaya C., 2010, An experimental study on steel-encased buckling restrained brace hysteretic damper, *Earthquake Engineering and Structural Dynamics*, **39**, 561-581
7. Fahnestock L.A., Sause R., Ricles J.M., 2007, Seismic response and performance of buckling-restrained braced frames, *Journal of Structural Engineering*, **133**, 9, 1195-1204
8. Fujimoto M., Wada A., Saeki E., Watanabe A., Hitomi Y., 1988, A study on the unbonded brace encased in buckling restraining concrete and steel tube, *Journal of Structural and Construction Engineering*, **34B**, 249-258
9. Inoue K., Sawaizumi S., Higashibata Y., 2001, Stiffening requirements for unbonded braces encased in concrete panels, *ASCE Journal of Structural Engineering*, **127**, 6, 712-719
10. Iwata M., Murai M., 2006, Buckling-restrained brace using steel mortar planks performance evaluations as hysteretic damper, *Earthquake Engineering and Structural Dynamics*, **35**, 1807-1826
11. Kato M., Usami T., Kasai A., 2002, A numerical study on cyclic elasto-plastic behavior of buckling-restraining brace members, *Journal of Structural and Construction Engineering*, **48A**, 641-648
12. Kinoshita T., Koetaka Y., Inoue K., Iitani K., 2007, Criteria of buckling-restrained braces to prevent out-of-plane buckling, *Journal of Structural and Construction Engineering*, **621**, 141-148
13. Korzekwa A., Tremblay R., 2009, *Behavior of Steel Structures in Seismic Areas*, Taylor & Francis Group, London, Chap. 94
14. Matsui R., Takeuchi T., Hajjar J.F., Nishimoto K., Aiken, I., 2008, Local buckling restraint condition for core plates in buckling-restrained braces, *Proceeding of 14th World Conference on Earthquake Engineering*, Beijing, China
15. Qiang X., 2005, State of the art of buckling-restrained braces in Asia, *Journal of Constructional Steel Research*, **61**, 727-748
16. Sabelli R., Mahin S., Chang C., 2003, Seismic demands on steel braced frame buildings with buckling-restrained braces, *Engineering Structures*, **5**, 655-666
17. Takeuchi T., Suzuki K., Marukawa T., Kimura Y., Ogawa T., Sugiyama T., 2005, Performance of compressive tube members with buckling restrained composed of mortar in-filled steel tube, *Journal of Structural and Construction Engineering*, **590**, 71-78
18. Tembata H., Koetaka Y., Inoue K., 2004, Out-of-plane buckling load of buckling restrained braces including brace joints, *Journal of Structural and Construction Engineering*, **581**, 127-134
19. Tremblay R., Bolduc P., Neville R, DeVall R., 2006, Seismic testing and performance of buckling restrained bracing systems, *Canadian Journal of Civil Engineering*, **33**, 1, 183-198
20. Usami T., 2006, *Guidelines for Seismic and Damage Control Design of Steel Bridges*, Japanese Society of Steel Construction, Gihodo-Shuppan, Tokyo, Japan
21. Watanabe A., Hitomi Y., Yaeki E., Wada A., Fujimoto M., 1988, Properties of braces encased in buckling-restraining concrete and steel tube, *Proceedings of 9th World Conference on Earthquake Engineering*, 719-724
22. Watanabe N., Kato M., Usami T., Kasai A., 2003, Experimental study on cyclic elasto-plastic behavior of buckling-restraining braces, *Journal of Earthquake Engineering*, **133**

Manuscript received December 5, 2012; accepted for print February 15, 2013